Developmental and Comparative Immunology 129 (2022) 104295

Contents lists available at ScienceDirect

Developmental and Comparative Immunology

journal homepage: www.elsevier.com/locate/devcompimm

DNA methylation in promoter region of immune related genes *STAT3* and *VEGFA* and biochemical parameters change in muscle of Japanese flounder under acute hypoxia

Xiaohui Li, Binghua Liu, Jun Yang, Guangling Li, Haishen Wen, Meizhao Zhang, Jifang Li, Feng He *

Key Laboratory of Mariculture, Ocean University of China, Ministry of Education, Qingdao, 266003, PR China

ARTICLE INFO

Keywords
Hypoxic stress
Muscle immunity
DNA methylation
Biochemical changes
Japanese flounder

ABSTRACT

Acute hypoxic stress can lead to immune response in fish, but the molecular mechanism of muscle immunity in fish under acute hypoxia are still unclear. In this study, we carried out the effect of signal transducer and activator of transcription3(*STAT3*) and vascular endothelial growth factor A(*VEGFA*) on muscle immune responses of Japanese flounder (*Paralichthys olivaceus*) during acute hypoxic stimulation (1.65 ± 0.28mg/L O_2; 3h, 6h, 12h, 24h) and reoxygenation (7.30 ± 0.40mg/L O_2; R12h, R24h, R48h). In situ hybridization (ISH) showed that *STAT3* and *VEGFA* RNA were co-located in the skeletal muscle of Japanese flounder. Japanese flounder was seriously affected by hypoxia for 3h and 6h. The expression of *STAT3* and *VEGFA* increased significantly. The methylation levels of *STAT3* 5′UTR region and *VEGFA* promoter region were significantly lower than those in normoxia group, which was negatively correlated with the expression levels of *STAT3* and *VEGFA*. The enzyme activities (LDH, ALT, AST, ALP) changed significantly. In addition, enzyme-linked immunosorbent assay (ELISA) detected a positive correlation between serum *VEGFA* concentration and muscle *VEGFA* mRNA. The current study have shown that Japanese flounder responded to acute hypoxic stress at multiple metabolic levels by changing DNA methylation status and activating transcription factors such as *HIF-1α*, *Nrf2* and *STAT3*. It is significant for the scientific development of aquaculture through analyzing the effects of hypoxia on biological immunity.

1. Introduction

Oxygen is the most essential element of hydrochemical environmental factors; it limits organisms' distribution and effects species diversity of their communities (Soldatov, 2012). Thousands of square km^2 of the world's oceans are affected by low oxygen levels, which can decimate marine animals and reduce fishing yields in many places (Wu, 2002). Hypoxia might promote a rapid increase in the generation of reactive oxygen species (ROS), which could in turn trigger oxidative stress in animals (Nam et al., 2020). It has been proved that hypoxia can regulate cellular immune activity physiologically and pathologically (Taylor and Colgan, 2017). In aquatic animals, hypoxia is associated with growth retardation, impaired immunity, susceptibility to pathogens, oxidative stress, and mortality, for example, hypoxia (2.5mg O_2 L^{-1}) reduces the immune response of abalone by reducing the total number of total hemocyte count, bacteriostatic activity, and lysozyme activity (Cheng et al., 2004; Nam et al., 2020). At present, there are few studies on the effects of acute hypoxic stress and reoxygenation on fish immunity.

As for the immune research, more focus on liver, spleen, kidney and other tissues, the immune research on muscle tissue is relatively less. In most organisms, skeletal muscles, which make up a large percentage of total body mass, consume a vast supply of energy in the form of ATP and stored fuel, such as glycogen and lipids (Ellen et al., 2008). Interestingly, skeletal muscle can also support a strong immune system, studies have shown that skeletal muscle antagonizes T cell exhaustion by protecting T cell proliferative potential from inflammation and replenishing the effector T cell progeny pool in lymphoid organs (Wu et al., 2020). Recently studies have shown that hypoxia/reoxygenation significantly modulated the expression of 96 genes governing various pro-inflammatory signaling including apoptosis in the rat skeletal muscle (Aravindan et al., 2010). In acute hypoxia, before

* Corresponding author. Ocean University of China, No 5 Yushan Road, Qingdao, 266003, PR China.
E-mail address: hefengouc@ouc.edu.cn (F. He).

https://doi.org/10.1016/j.dci.2021.104295
Received 4 September 2021; Received in revised form 9 October 2021; Accepted 12 October 2021
Available online 15 October 2021
0145-305X/

acclimatization has time to take place, the rat microvasculature, including skeletal muscle microvessels, has been reported to experience a rapid inflammatory response (Ellen et al., 2008), ROS can induce the release of *VEGF* through the PI3K/AKT pathway, *HIF-1α* and *STAT3* were identified as the most important transcription factors to activate the *VEGF* promoter region (Kosmidou et al., 2001; Xu et al., 2005). In this study, acute hypoxia (3h, 6h, 12h, 24h) and reoxygenation (12h, 24h, 48h) were performed on Japanese flounder. Flounder is an important benthic Marine fish and is widely farmed in Japan, Korea and China.

STAT3/VEGF is an immune-related signaling pathway, and hypoxia increases the activation of *STAT3* and up-regulates the expression of *VEGFA* genes (Sarma et al., 2016). *VEGF* could be directly regulated by p-*STAT3* (Cao et al., 2015). The activated *STAT3* binds to hypoxia-related elements in the promoter region of *VEGFA* and transcriptionally regulates the gene expression of *VEGFA*. *STAT* (signal transducers and activators of transcription)proteins are latent transcription factors that become activated by phosphorylation on a single tyrosine (near residue 700), typically in response to extracellular ligands (Jr, 1997; Stark et al., 1998). Subsequently, *STAT* proteins are recruited to the receptor-JAK complexes and activated by tyrosine phosphorylation, which promotes the formation of homodimers or heterodimers of *STAT* family members. Activated *STATs*, in turn, translocate to the nucleus and bind to specific DNA response elements that regulate gene expression (Turkson et al., 1998). Vascular endothelial growth factor (*VEGF*) is a hypoxia inducible secreted protein that interacts with receptor tyrosine kinases on endothelial cells to promote angiogenesis (Jin et al., 2002). The expression of *VEGF* is potentiated in response to hypoxia, by activated oncogenes, and by a variety of cytokines (Gera et al., 1999). Additional mechanisms induced during hypoxic exposure that could signal skeletal muscle *VEGF* activation include inflammation, possibly linked to reactive O_2 species generation, or a change in cellular energy status as reflected by AMP kinase activity (Ellen et al., 2008). In many studies, environmentally induced changes in gene expression are associated with altered DNA methylation patterns or with altered histone modifications (Feil and Fraga, 2012). To date, much of the focus in 'environmental epigenetics' has been on DNA methylation (Feil and Fraga, 2012).

At present, no relevant studies have been reported on the *STAT3/VEGFA* signaling pathway in skeletal muscle under acute hypoxic stress and reoxygenation. Therefore, this study aimed to investigate the expression and regulation mechanism of skeletal muscle *STAT3* and *VEGFA* under acute hypoxic stress and reoxygenation, so as to provide a reasonable basis for guiding aquaculture.

2. Materials and methods

2.1. Ethics statement

All Japanese flounder were treated in accordance with the guidelines of animal Research and Ethics Committee of Ocean University of China, and no endangered or protected species were found.

2.2. Experimental fish and data collection

Healthy Japanese flounder were supplied by Qingdao Haoruiyuan Aquaculture Seedling limited company. All Japanese flounder are raised for three days to acclimate to the sea water and are replaced daily during the acclimation period. Water temperature was maintained at 18.47 ± 0.47 °C (range: 17.5–19.3 °C), dissolved oxygen in water was maintained at 7.52 ± 0.17mg/L (range: 7.13–7.91mg/L), and pH value in water was maintained at 6.05 ± 0.10 (range: 5.8–6.2), the salinity of seawater is maintained at 29.08 ± 0.35 ppt (range: 28–30 ppt), and 14:10h light: dark period. In addition, during the adaptation period, all flounder were fed once a day at 5:00 p.m. until 24 hours before the experiment. The experimental period was divided into the experimental group and the control group: the experimental group was subjected to acute hypoxic stress (1.65 ± 0.28mg/L O_2 (range: 1.10–2.08mg/L)), and the normal oxygen level (7.30 ± 0.40mg/L O_2 (range: 6.60–8.19mg/L)) was restored after 24h of hypoxic stress. Three flounder were randomly selected for 0h, 3h, 6h, 12h, 24h under hypoxic conditions and 12h, 24h and 48h under reoxygenated conditions, respectively, and a total of 27 flounder were obtained. The flounder was anesthetized with anaesthetic powder (tricaine methane sulfonate; MS-222; 200mg/L)before sampling. The body weight and body length were measured. Blood samples were collected from the tail vein of Japanese flounder using a syringe. The serum obtained was separated (5000 rpm/min, 10min, 4 °C)and the supernatant collected was stored in −80 °C. The collected tissue was immediately placed in liquid nitrogen and stored at −80 °C until treatment.

2.3. Genetic structure and phylogenetic analysis of STAT3 and VEGFA

Online methylation substrate design software (http://www.urogene.org/methprimer/)was used to locate CG-rich regions, and JASPA software (http://jaspar.genereg.net/) was used to predict transcription factor binding sites. The amino acid sequences of *STAT3* and *VEGFA* were obtained from NCBI(Fig. 1). The phylogenetic tree was constructed in molecular evolutionary genetics analysis software (MEGA 7.0), and the topological stability of the tree was evaluated with Neighbor-Joining (NJ) method (under 1000 bootstrap replications).

2.4. RNA isolation and qPCR

Total RNA extraction reagent Trizol (Vazyme, China) was used to extract total muscle RNA at each time point. The RNA concentration of each sample was measured by enzyme plate analyzer, and the RNA concentration of each sample was diluted to 500ng/ul to facilitate reverse transcription experiments. RNA integrity was checked by agarose gel electrophoresis. RNA reverse transcription was performed using HiScript III RT Supermix for qPCR(+gDNA wiper) kit (Vazyme, China). The total reaction system was 20ul, including two parts: genomic DNA removal, 4ul 4x gDNA, 1ul RNA template, 11ul RNase-free ddH_2O, 42 °C, 2min; reverse transcriptional reaction: 4ul 5xHiScript III QRT Supermix was added to 16ul reaction solution at 37 °C for 15min,85 °C for 5sec in an upward step. The cDNA was stored at −20 °C.

2.5. Quantitative real-time PCR(qPCR)

Quantitative real-time PCR was conducted by the Roche LightCycler480 (German) with ChamQTM SYBR ® Color q-PCR Master Mix (High ROX Premixed) (Vazyme, China). The expression levels of target genes *STAT3* and *VEGFA* and reference gene 18S were determined, quantitative primers are shown in Table 1(18S primer was referred to (Wu et al., 2018). The 10ul mixture of PCR consisted of 5ul SYBR ®Premix Ex Taq, 0.2ul upstream primers, 0.2ul downstream primers, 1ul cDNA template, and 3.6ul ddH_2O. PCR program was as follows: 95 °C for 30 s, followed by 40 cycles of denaturation at 95 °C for 10 s, 60 °C for 30s and 72 °C for 15 s. Each sample was run in triplicates and the relative expression of the target gene was calculated by $2^{-\Delta\Delta Ct}$ method (Livak and Schmittgen, 2001).

2.6. In situ Hybridization(ISH)

In situ hybridization was performed using frozen sections. The skeletal muscle of Japanese flounder were removed and fixed in buffered 4% paraformaldehyde for 24 h and then embedded in saccharose (Kanda et al., 2011). Seven-micron-thick sections were cut for ISH. In situ hybridization with cDNA extends the DNA sequence of *STAT3* and *VEGFA* gene. In-situ hybrid primers are shown in Table 2. Three protective bases and SP6 promoter sequences were added to the forward primer front end, and three protective bases and T7 promoter sequences were added

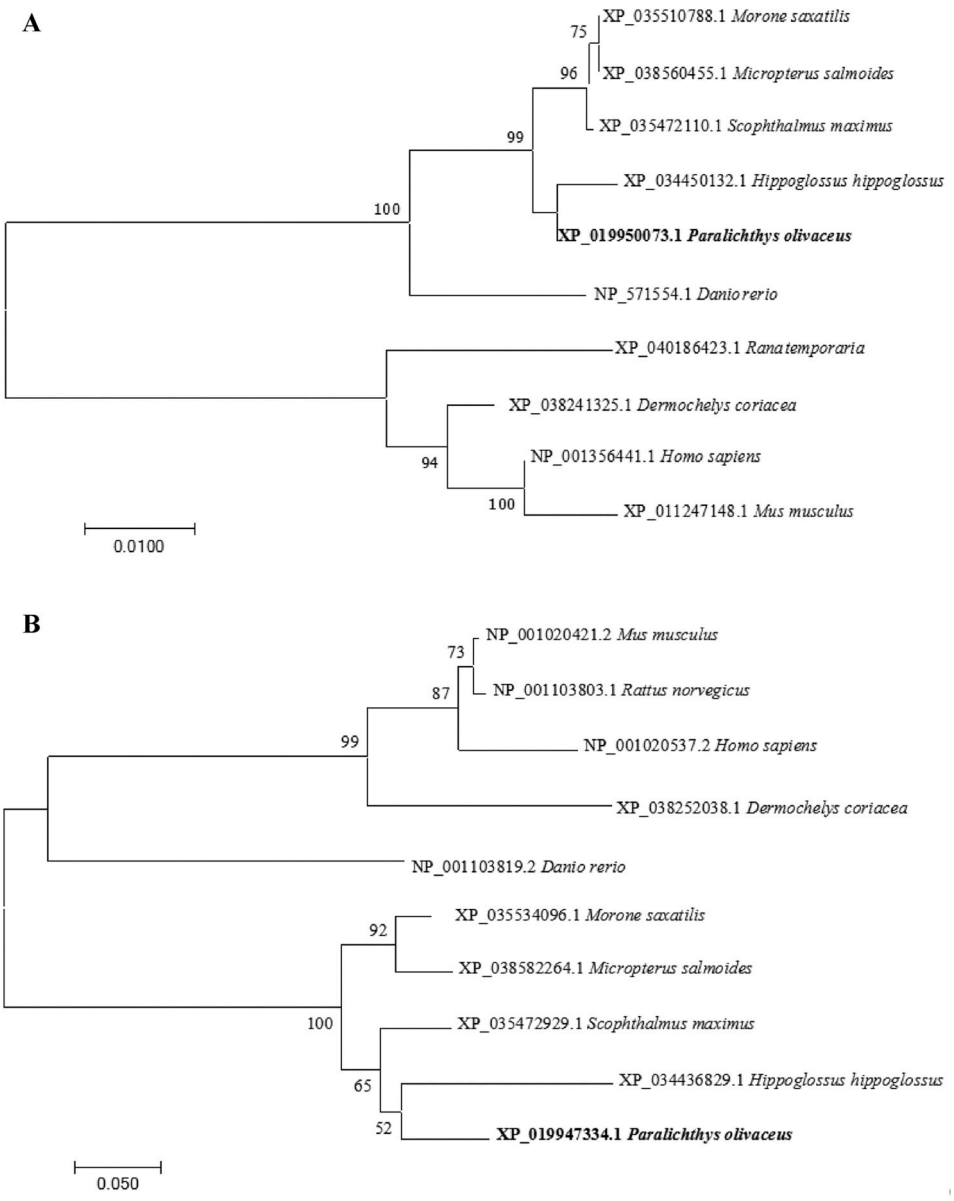

Fig. 1. Phylogenetic trees of *STAT3* and *VEGFA* proteins. The percentage of replicate trees in which the associated taxa clustered together in the bootstrap test (1000 replicates) are shown next to the branches. The tree is drawn to scale, with branch lengths in the same units as those of the evolutionary distances used to infer the phylogenetic tree. The target species are indicated in bold. (A) Phylogenetic tree of *STAT3* proteins. (B) Phylogenetic tree of *VEGFA* proteins.

Table 1
Primers used for q-PCR.

Primer name	Sequence (5′-3′)	Product size (bp)	Tm (°C)	Accession no.
STAT3-RT	F:AGGTTGCTGAGGTGCTAA R: TGATCTGACAGCCAGAGTAG	126	60.0	XM_020094516.1
VEGFA-RT	F: CTGTCAAGAGCGCCCACATA R: CGGGATGAAGATGTGCTCCA	158	60.0	XM_020091775.1
18S-RT	F: ATTGACGGAAGGGCACCAC R: ATGCACCACCACCCACAGA	134	60.0	EF126037.1

to the reverse primer front end. In situ hybrid probe (603bp) for the digoxin-labeled *STAT3* gene and in situ hybrid probe (507bp) for the biotin-labeled *VEGFA* gene.

The sections were washed by 1xPBS, sealed by 3%H_2O_2, digested by protease K (10ug/ml), and deionized after 1h pre-hybridization at 52 °C without riboprobe, and then hybridized at 52 °C for 20h with riboprobe. After hybridization, sections were washed in 5*SSC (preheating), 5*SSC, 2*SSC, 1*SSC and 0.2*SSC for 15min; 1xPBS for 5 min; 1*blocking buffer (Roche Diagnostics, Germany) for 30 min; Digoxin (DIG) antibody (Roche Diagnostics, Germany) was incubated for 1h; 1xPBS for 4*10min; 488-Alexa Fluor (green, Roche Diagnostics, Germany) coloration for 1h; 1xPBS for 2*5min; seal with 3%H_2O_2 for 20 min; 1xPBS for 5min; endogenous biotin blocking solution was sealed for 10 minutes; 1xPBS for 5min; 1*blocking buffer (Roche Diagnostics, Germany) for 30min; Biotin (Bio) antibody (Roche Diagnostics, Germany) was incubated for 1h; 1xPBS for 4*10min; 594-Alexa Fluor (red, Roche Diagnostics, Germany)coloration for 1h; 1xPBS for 2*5min; DAPI staining the nucleus for 5s; 1xPBS, 2*5min. The sections were sealed with

Table 2
Primers used for double in situ hybridization.

Primer name	Sequence (5′-3′)	Product size (bp)	Tm (°C)	Accession no.
STAT3-ISH	F:cgcatttaggtgacactatagaagcgTCCATCCTGTGGTACAACATGC R:ccgtaatacgactcactatagggagacaCTTGTAGCCCATGATGATGTCG	603	60.0	XM_020094516.1
VEGFA-ISH	F:cgcatttaggtgacactatagaagcgCTGTCAAGAGCGCCCACATA R:ccgtaatacgactcactatagggagacaTCGGCTTGTCACATTTGCAG	507	60.0	XM_020091775.1

blocking reagent for antibody incubation and fluorescence color development. After that, the slices were sealed and observed under fluorescence microscope.

2.7. Genomic DNA isolation, DNA bisulfite modification and analysis

Genomic DNA was extracted from skeletal muscle of flounder using Marine animal genomic DNA kit (TIANGEN, China). 0h, 3h, 6h, 12h of hypoxia were required to extract genomic DNA of the three Japanese flounder at each time point. Genomic DNA integrity was determined by agarose gel electrophoresis. Store at −20 °C until use.

Genomic DNA was modified using the BisulFlash DNA Modification Kit (EpiGentek, USA) following the manufacturer's instructions. Primers were designed on Oligo 6.0 based on bisulfate modified DNA sequences. Methylation specific PCR was performed (Takara, Japan), and the PCR products were separated by agarose gel electrophoresis (Table 3). The purified products were obtained by using the gel recovery kit (Vazyme, China). The purified product was cloned into pCE_2TA/Blunt-Zero vector (Vazyme, China) and transferred into DH5α Chemically Competent Cells. Three biological replicates were performed at each time point, and 10 clones were sequenced to evaluate the methylation level. The efficiency of bisulfite modification was calculated by the percentage of transformed cytosine to total cytosine (except CpG dinucleotide cytosine).

2.8. Biochemical index(LDH, AST, ALT, ALP)and VEGFA detection

The skeletal muscle is thawed on ice, skeletal muscle (1-time mass, g) and normal saline (9-times volume, mL) were mixed in an eppendorf tube and ground fully in a Tissue Grinder (DHS, China). Then, 10% muscle tissue homogenate was obtained after centrifugation (5000 rpm, 10 min, 4 °C) and discarding sediment. Lactate dehydrogenase (LDH), aspartate aminotransferase (AST), alanine aminotransferase (ALT), alkaline phosphatase (ALP) activity were detected with the kit. In addition, fresh blood was centrifuged at 4 °C for 10 min at 5000 rpm to obtain serum and the protein content of *VEGFA* was detected by the kit (BYBIO, China).

2.9. Statistical analysis

Data is represented in the average ± standard difference. Statistical differences were analyzed using single factor variance analysis (one-way ANOVA) and Duncan's multiple range test (SPSS 25.0) (Tian et al., 2018). The Pearson correlation coefficient between mRNA expression levels and methylation levels was tested by independent sample. $P < 0.05$ is significant.

3. Results

3.1. Phylogenetic analysis

In order to study the evolutionary relationship between *STAT3* and *VEGFA* proteins in flounder and other species, and to prove that *STAT3* and *VEGFA* proteins have the same function with other species proteins, phylogenetic tree was constructed by MEGA7.0 software, and amino acid sequences of 10 species were analyzed. The clustering results were shown in Fig. 1. The percentage of replicate trees in which the associated taxa clustered together in the bootstrap test (1000 replicates) are shown next to the branches, and percentages represent the reliability of the branches of the phylogenetic tree. The amino acid sequences of *STAT3* and *VEGFA* can be divided into two branches, namely fish and other vertebrates. The two groups of organisms close to the fulcrum are closely related by evolution. *STAT3* protein and *VEGFA* protein were conserved in the system evolution.

3.2. Double in situ hybridization of STAT3 and VEGFA RNA in skeletal muscle

The *STAT3* and *VEGFA* RNA distribution in the muscle was determined by ISH. Tissue sections were made from skeletal muscle of Japanese flounder and ISH was detected. The localization of *STAT3* and *VEGFA* RNA in skeletal muscle is shown in Fig. 2. The locations of *STAT3* RNA, *VEGFA* RNA and nucleus in skeletal muscle cells of Japanese flounder were observed, and it was found that *STAT3* RNA and *VEGFA* RNA co-existed near muscle nucleus. In order to further verify this result, the three observation images were combined together. After careful observation, it was found that *STAT3* RNA and *VEGFA* RNA were co-expressed near the nucleus of skeletal muscle cells of Japanese flounder.

3.3. DNA methylation status of STAT3 under acute hypoxia

DNA methylation levels of two sequences (S1: 556∼-277, 279bp S2: 305∼-133, 172bp) in CG island (CG: 485∼-120, 365bp) of *STAT3* gene promoter and 5′UTR were detected. When relative profile score threshold is above 98%, the trascription factors and their binding sites about *STAT3* S1 were shown in Fig. 3A. The 11 transcription factors in the S1 region include Arid3a, CREB1, Atf3, FOXO6, FOXO4, FOXL1, FOXI1, FOXD2, FOXP3, CREB1, CREB1. When relative profile score threshold is above 95%, the trascription factors and their binding sites about *STAT3* S2 were shown in Fig. 3B. S2 region have 10 transcription factors, including NFIC, TBX4, TBX5, GATA5, GATA3, TBX6, TBX3, Ahr: Arnt, GATA2, GATA3. To evaluate the efficiency of the bisulfite modification step, 12 different samples were selected to detect the conversion

Table 3
Primers used for bisulphate PCR (BS-PCR).

Primer name	Sequence (5′-3′)	Product size (bp)	Tm (°C)	Accession no.
STAT3-BS1	F1:ATAGATATTTTGATTGGTTGTAGTGG R1:AAAATAACAAAAACTCCTTTCCTATC	172	50.8	XM_020094516.1
STAT3-BS2	F2:GTGATTGAAGGTTGATTAGTAAAGA R2:CCACTACAACCAATCAAAATATCTA	278	50.0	XM_020094516.1
VEGFA-BS	F:GAGGATATATTTATTATTTTTAGAAG R:ATTTATACTCCTATATACAATCTAAA	280	42.0	XM_020091775.1

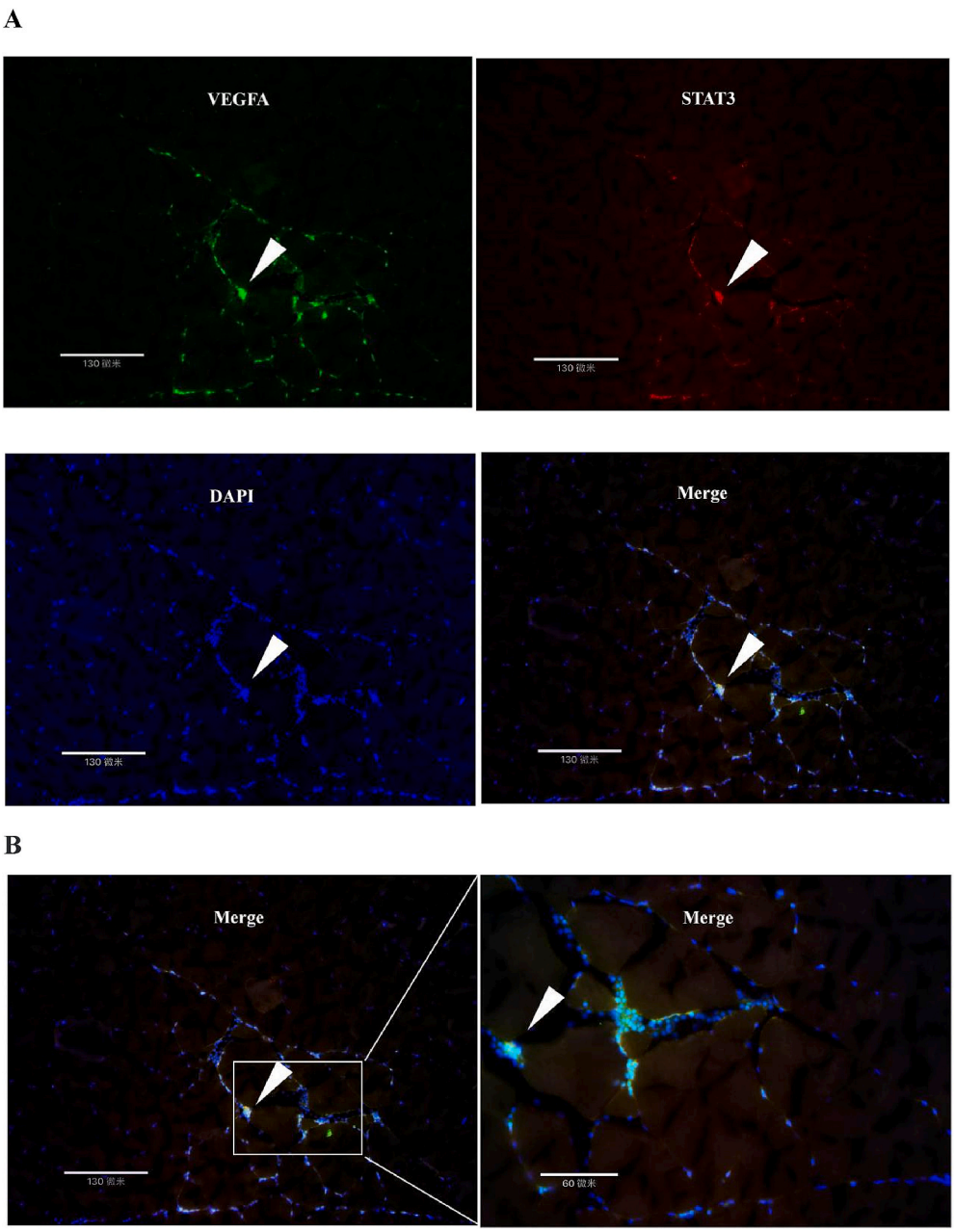

Fig. 2. In situ hybridization of *STAT3* and *VEGFA* mRNA was co-located. (A) The double in situ hybridization (D-ISH) result of *STAT3* and *VEGFA* RNAs in skeletal muscle. (B) Amplified figure of double in situ hybridization (D-ISH) result of *STAT3* and *VEGFA* RNAs in skeletal muscle.

of 62 and 46 cytosine except cytosine in CpG dinucleotide. The sequencing results showed that almost all cytosine was modified into uracil by bisulfite. The conversion efficiency was above 95%, this indicating that bisulfite treatment was effective. By analyzing the methylation levels of S1 and S2 regions, it was found that both regions showed hypomethylated levels (S1 and S2: 3.625 ± 0.481%). With the change of hypoxia time, the methylation level decreased at 0–6 hours (from (4.06 ± 1.75)% to (2.90 ± 0.41)%, $P > 0.05$) and increased at 6–12 hours (from (2.90 ± 0.41)% to (4.06 ± 0.41)%, $P > 0.05$) (Fig. 4A). It is noteworthy that there were significant changes ($P < 0.05$) in methylation levels in 5 'UTR region of S2 region. After 3h and 6h hypoxia, the 5 'UTR methylation level in the S2 region was significantly lower ($P < 0.05$) than that in the normoxic group (Fig. 5A). In addition, we also analyzed the methylation levels of single CpG sites in the S1 and S2 regions of *STAT3*, and found different trends. Among the 18 CpG sites in *STAT3*, trend of rising first and then decreasing appeared at the site of −499, −236, −195, −159; decreasing first and rising then at −430, −375, −270, −257. The methylation levels of other CpG sites decreased or increased with the time of hypoxia.

3.4. DNA methylation status of VEGFA under acute hypoxia

DNA methylation levels of one sequence (S3: 679∼-399, 280bp) in CG island (CG: 679∼-401, 278bp) of *VEGFA* gene promoter were detected. When relative profile score threshold is above 95%, the transcription factors and their binding sites about *VEGFA* S3 were shown in Fig. 3C. S3 region have 9 transcription factors, including ZEB1, ZNF354C, Nkx2-5, E2F1, MZF1, Tcfl5, Zic1:Zic2, Atoh1, GATA3. To evaluate the efficiency of the bisulfite modification step, 12 different samples were selected to detect the conversion of 60 cytosine except cytosine in CpG dinucleotide. The conversion efficiency was above 96%, this indicating that bisulfite treatment was effective. The S3 region

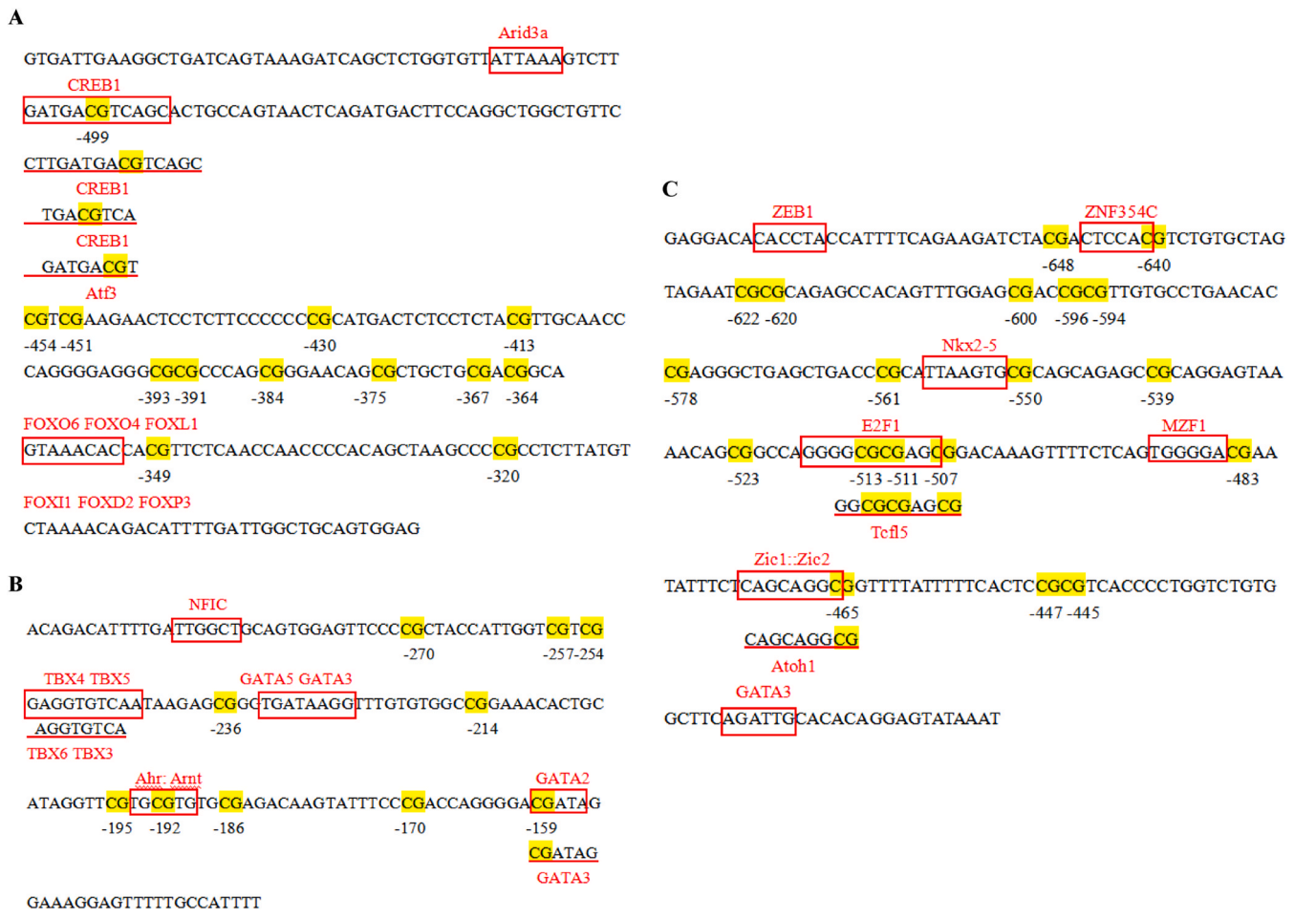

Fig. 3. The predictive transcription factors and putative binding sites. (A, B) Predictive transcription factors and putative binding sites on the *STAT3* promoter and 5′UTR. (C) Predictive transcription factors and putative binding sites on the *VEGFA* promoter. The CpG dinucleotide sites are represented by the yellow shade. The red frames represent the putative binding sequences of the transcription factors and the predictive transcription factors are indicated above them.

showed hypomethylation level (S3: 4.08 ± 1.95%). With the change of hypoxia time, the methylation level decreased at 0–6 hours (from (6.49 ± 1.08)% to (1.75 ± 1.08)%, $P < 0.05$) and increased at 6–12 hours (from (1.75 ± 1.08)% to (5.44 ± 0.66)%, $P < 0.05$) (Fig. 4B). There were significant changes in methylation levels in S3 region. The methylation level of S3 region was significantly lower than that of normoxic group after hypoxia for 6h, and did not return to the methylation level of normoxic group after hypoxia for 12h (Fig. 5B). The methylation level of single CpG site in *VEGFA* was analyzed, and found different trends. Among the 19 CpG sites in *VEGFA*, trend of rising first and then decreasing appeared at the site of −523, −511, −465, −445; decreasing first and rising then at −648, −640, −594, −578, −507 (Table 4).

3.5. The regulatory relationship of STAT3 and VEGFA

Fig. 6 showed the expression levels of *STAT3* and *VEGFA* in different stages of hypoxia. Compared with the control group, the relative expression level of *STAT3* mRNA was significantly increased at 3h, 6h and 24h of hypoxia, and at 12h and 24h of reoxygenation. The relative expression level of *STAT3* mRNA was the highest at 3h and 6h of hypoxia, while the relative expression level of *STAT3* mRNA was not significantly increased at 12h of hypoxia. In addition, compared with the control group, the relative expression of *VEGFA* mRNA was significantly increased at 3h and 6h, and there was no significant increase at 12h, 24h and 12h after hypoxia, while the mRNA expression of *VEGFA* decreased slightly at 24h after reoxygen. Then linear regression was used to analyze the relationship between the methylation level of S2 5′UTR region and the expression level of *STAT3*, as well as the relationship between the methylation level of S3 region and the expression level of *VEGFA*. The results showed that the *STAT3* expression level was negatively correlated ($Y = -4.1657x+5.2845$, $R^2 = 0.4312$) with the 5 ‘UTR region methylation level of S2 (Fig. 7A), and the *VEGFA* expression level was also negatively correlated ($Y = -3.1391x+9.3445$, $R^2 = 0.656$) with the S3 region methylation level (Fig. 7B). In addition, the relationship between the methylation level of a single CpG site and the gene expression level was analyzed (Table 4), and it was found that the methylation level of −445, −447, −511 and −622 sites in the S3 region was negatively correlated with the expression level of *VEGFA*.

The study found that the changes in *STAT3* and *VEGFA* expression levels were related to the duration of hypoxia. Under different hypoxia and reoxygenation conditions, the change trend of *STAT3* expression level was consistent with that of *VEGFA* expression level, which increased first and then decreased (Fig. 8). Compared with normoxic group, the expression level was significantly increased at 3h and 6h hypoxia. Linear regression analysis showed that there was a positive correlation between *STAT3* expression and *VEGFA* expression under different conditions of hypoxia and reoxygenation ($Y = 0.3497x+0.2126$, $R^2 = 0.562$).

3.6. Biochemical indices during acute hypoxia

LDH exists widely in skeletal muscle, and the activity of LDH increases when skeletal muscle is damaged. The activity of LDH increased (from hypoxia 0–3h) first and then decreased (from hypoxia 3h to

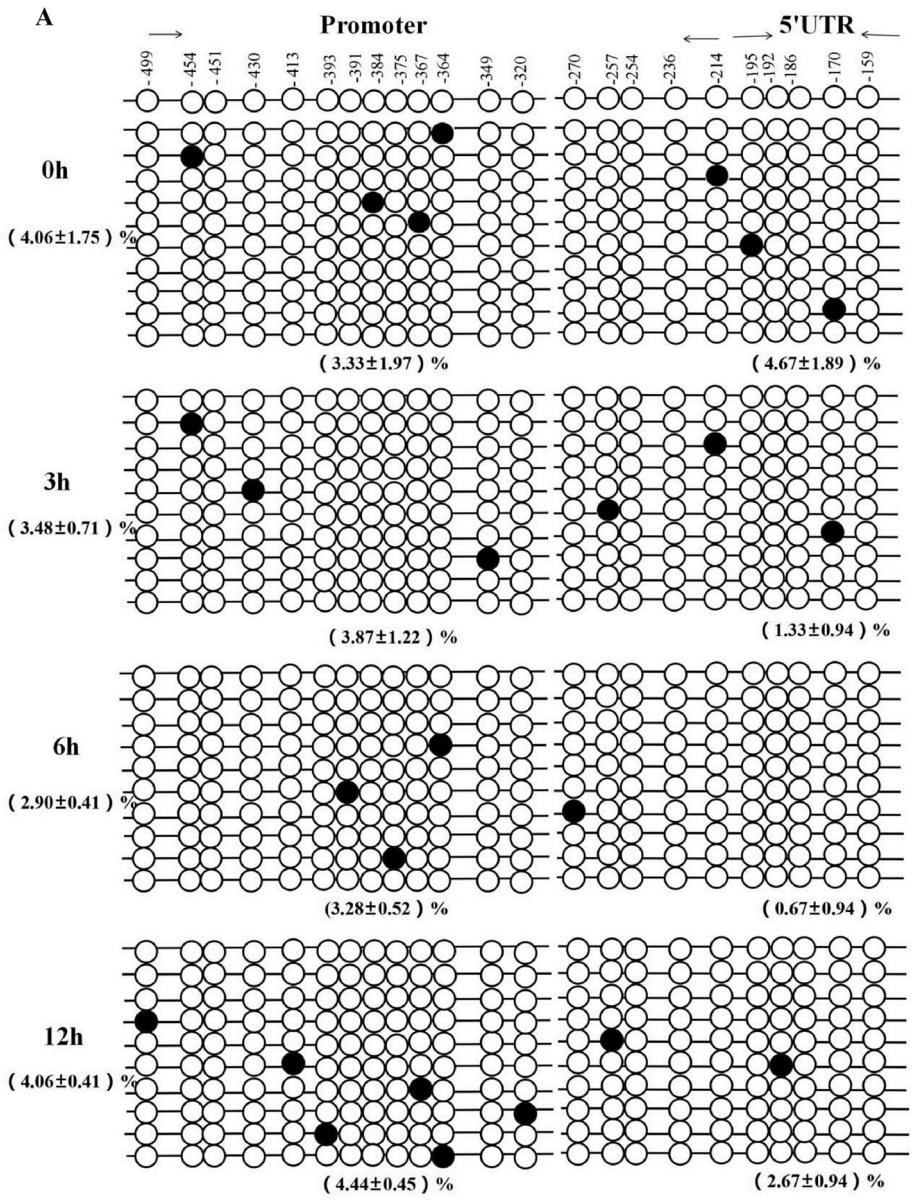

Fig. 4. DNA methylation patterns of *STAT3* and *VEGFA*. (A) DNA methylation patterns of *STAT3*. (B) DNA methylation patterns of *VEGFA*. ○ represents an unmethylated CpG, and ● represents a methylated CpG. Each line represents the methylation status of all CG sites in a clone. The percentage indicates the average methylation level (under the line) of all clones of each hypoxia time point, calculated as the number of methylated CpG sites per total number of CpG sites in each stage, data as mean ± SEM.

reoxygenated 48h). Except for 3h hypoxia group, there was no significant difference in the concentration of each group, and the activity of LDH in 3h hypoxia group was significantly higher ($P < 0.05$) than that in normoxia group (Fig. 9A). ALT and AST are two of the most important transaminases, which play an important role in promoting metabolism. antioxidant enzymes. The activity of ALT increased firstly (from hypoxia 0h–3h), then decreased (from hypoxia 3h–24h) and then increased (from hypoxia 24h to reoxygenated 48h). ALT concentration was shown in Fig. 9B, in which significant differences between control and hypoxia treatment occurred in 3h and reoxygenated for 24 and 48h group ($P < 0.05$). The activity of AST increased firstly (from hypoxia 0h–6h), then decreased (from hypoxia 6h–12h) and then increased (from hypoxia 12h to reoxygenated 48h). In Fig. 9C, the results showed that the concentration of AST was significantly increased ($P < 0.05$) when hypoxia 6h and reoxygenated for 24 and 48h. In addition, There was no significant difference in concentration between each group and normoxia group. Under hypoxia and reoxygenation treatment, the overall trend of AST and ALT concentration was a process of first increase, then decrease and then increase. It is particularly noteworthy that AST concentration had a minimum value at 12 hours of hypoxia, and ALT concentration had a minimum value at 24 hours of hypoxia, but there was no significant difference between the two groups ($P > 0.05$). ALP is an important regulatory enzyme in animal metabolism and is a non-specific hydrolase. Under hypoxia and reoxygenation, as show in Fig. 9D, the overall trend of ALP is to decrease (from hypoxia 0h–12h) first and then increase (from hypoxia 12h to reoxygenation 48h), and the activity of ALP in hypoxia group at 6h, 12h and 24h is significantly lower than that in normoxia group ($P < 0.05$), and there is no significant difference between ALP activity and normoxia group after reoxygenation.

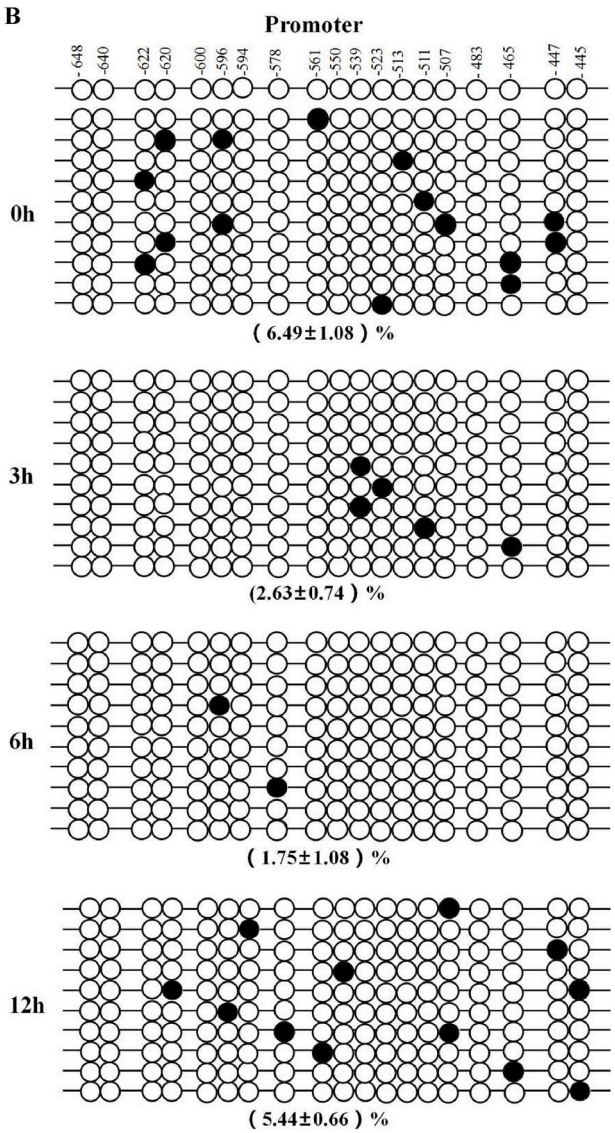

Fig. 4. (*continued*).

3.7. VEGFA protein concentration and VEGFA mRNA expression under acute hypoxia

In order to determine whether hypoxia and reoxygenation treatment would affect *VEGFA*, serum *VEGFA* concentration was measured. Results as shown in Fig. 10, *VEGFA* concentration changes of the whole is the trend of the rise and fall first and found that the concentration of serum *VEGFA* in hypoxia 3h group has the maximum significant differences with normoxia groups ($P < 0.05$). Interestingly, there was a strong correlation ($Y = 0.0072x+0.2873$, $R^2 = 0.6131$) between serum *VEGFA* protein concentration and the relative expression of *VEGFA* mRNA in muscle with the duration of hypoxia (Fig. 11).

4. Discussion

Acute or chronic hypoxic stress may disturb physiological homeostasis and adversely affect the growth and health of fish (Abdel-Tawwab et al., 2015). In an anoxic environment, fish may undergo a variety of behavioral responses to better adapt to the environment. Hypoxia can affect the behaviour, growth, food consumption and physiological state of fish (Li et al., 2018). For example, hypoxic stress can negatively affect the growth performance and immunity of Nile tilapia (*Oreochromis niloticus*) (Abdel-Tawwab et al., 2015). *JAK/STAT3* is a classic inflammatory pathway, which is activated by hypoxia in rats and humans to produce inflammatory responses (Ortega et al., 2017; Wang et al., 2013). *VEGF* is a sensitive gene to hypoxia, and hypoxia can promote the expression of *VEGF* gene in puffer fish (*Tetraodontidae*) and mandarin fish (*Siniperca chuatsi*) (He et al., 2019; Li et al., 2019). Analysis of the protein phylogenetic tree revealed that the *STAT3* and *VEGFA* protein molecules associated with hypoxic stress were conserved during evolution. These results indicated that the *STAT3* protein and *VEGFA* protein functions of *Paralichthys olivaceus* may be consistent with those of other species. Therefore, *STAT3* and *VEGFA* genes under hypoxia were studied at the RNA level.

STAT3 RNA and *VEGFA* RNA were co-localized in skeletal muscle cells of Japanese flounder by in situ hybridization. In the study of ARPF-19 cells, it was found that hypoxia could activate the activation of *STAT3* and induce the expression of *VEGF* in ARPF-19 cells (Hwang et al., 2020). These results indicated that the expression of *STAT3* and *VEGF* was likely to be similar to that of ARPF-19 under hypoxic conditions. Therefore, the expression levels of *STAT3* and *VEGFA* under different hypoxic conditions were detected in this experiment. In this study, it was found that the change of *STAT3* gene expression at mRNA level was positively correlated with the change of *VEGFA* mRNA level, the

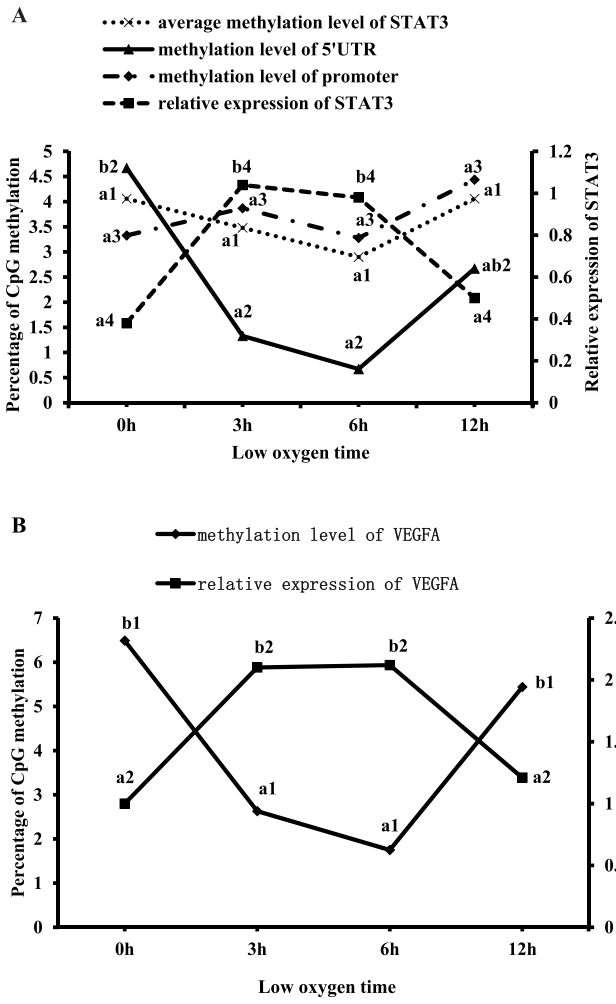

Fig. 5. DNA methylation levels and relative expression levels. (A) The correlation between DNA methylation levels and relative expression levels of *STAT3*. (B) The correlation between DNA methylation levels and relative expression levels of *VEGFA* at four hypoxia time points of Japanese flounder. Significant differences between stages are indicated by different letters.

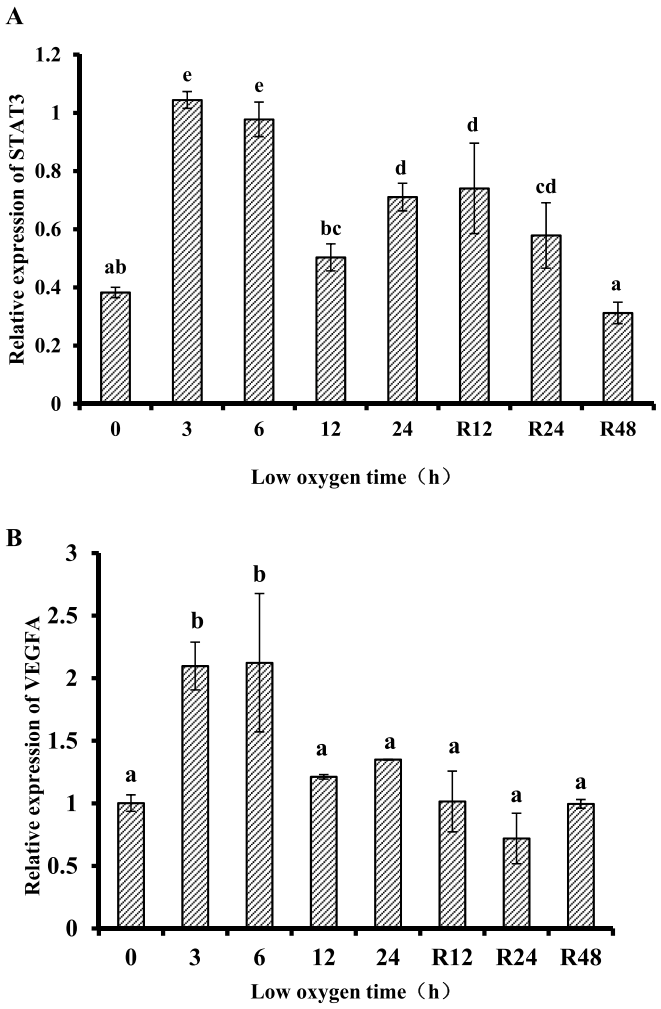

Fig. 6. Skeletal muscle mRNA expression at different hypoxia time point. (A, B) Skeletal muscle mRNA expression of *STAT3* and *VEGFA* in of Japanese flounder at different hypoxia time point. Each histogram represents the mean of three determinations. Values are expressed as mean ± standard error of mean. The mean values of each group were arranged in order from the smallest to the largest, marked a on the minimum mean, and then marked with letters in order of significance. Those with one same marked letter were considered insignificant, and those without the same marked letter were considered significant ($P < 0.05$, one-way ANOVA, followed by Duncan's test).

Table 4
Linear regression analysis results between expressions and methylation levels of *VEGFA* 19 CpG dinucleotides.

CpG site	R^2	P	Significant level	Function
−648	0.568	0.596	n.s.	–
−640	0.0526	0.441	n.s.	–
−622	0.7066	0.001	**	Y = −0.0314x+1.7267
−620	0.9107	0.250	n.s.	–
−600	0.8584	0.802	n.s.	–
−596	0.5400	0.532	n.s.	–
−594	0.2369	0.487	n.s.	–
−578	0.0848	0.416	n.s.	–
−561	0.7294	0.627	n.s.	–
−550	0.2018	0.728	n.s.	–
−539	0.4617	0.596	n.s.	–
−523	0.4554	0.330	n.s.	–
−513	0.9954	0.219	n.s.	–
−511	0.2544	0.006	**	Y = −0.1833x+1.9167
−507	0.4603	0.219	n.s.	–
−483	~0.000	–	n.s.	–
−465	0.7414	0.067	n.s.	–
−447	0.9967	0.019	*	Y = −0.2222x+2.1319
−445	0.0119	0.012	*	Y = −0.0314x+1.7267

The word n.s. indicates $P > 0.05$, and the signs *, ** represent $P < 0.05$, $P <$ 0 0.01, respectively. Furthermore, "~0.000" means value < 0.0001.

expression level of *STAT3* was significantly increased at 3h and 6h hypoxia. Previous studies have found that hypoxic stimulation increases *STAT3* activation in mesenchymal stem cells, and that *STAT3* not only mediates the partial production of *VEGF* under normoxia, but also mediates *VEGF* release in mesenchymal stem cells after hypoxic stimulation (Wang et al., 2007).

VEGF is an angiogenic factor closely related to angiogenesis and a typical oxygen sensitive gene, which plays a crucial role in physiological and pathological angiogenesis (Bautista et al., 2009). Hypoxia can up-regulate the expression of *VEGF* in lung epithelial cells, renal brain and astrocyte (Christou et al., 1998; Minchenko et al., 1994). *VEGF* is a regulator of innate immunity and has immunosuppressive effect (Turkowski et al., 2017; Yang et al., 2018). In this study, the effect of hypoxia on *VEGFA* mRNA expression in skeletal muscle of flounder was studied, and it was found that hypoxia caused the increase of *VEGFA* gene expression level, and *VEGFA* expression was significantly increased after 3 hours of hypoxia and 6 hours of hypoxia. This is similar to studies of hypoxia in rat type I astrocytes (Ijichi et al., 1995). Similarly, in the study of Amazon fish, the level of *VEGF* transcript was significantly

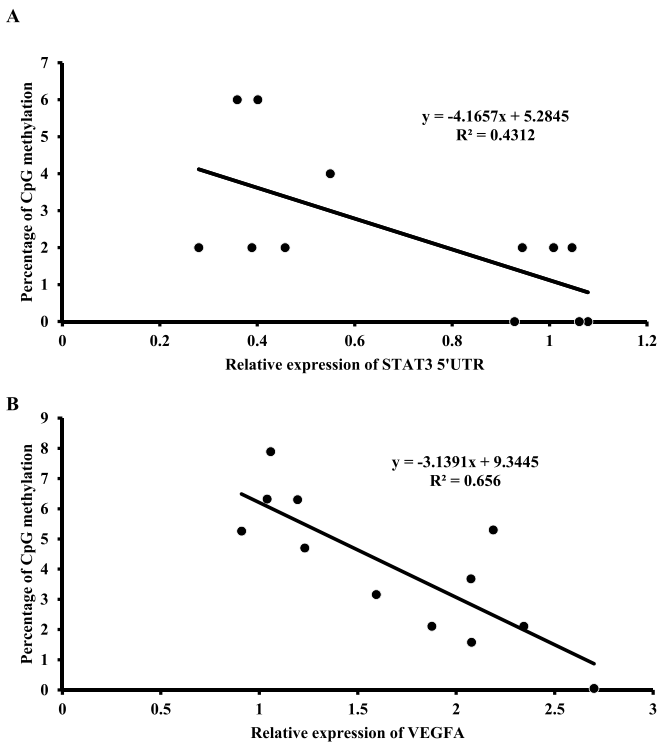

Fig. 7. Correlation between DNA methylation and gene expression. (A) The relationships between *STAT3* mRNA relative expressions and methylation levels of promoter by linear regression analysis. (B) The relationships between *VEGFA* mRNA relative expressions and methylation levels of 5′UTR by linear regression analysis.

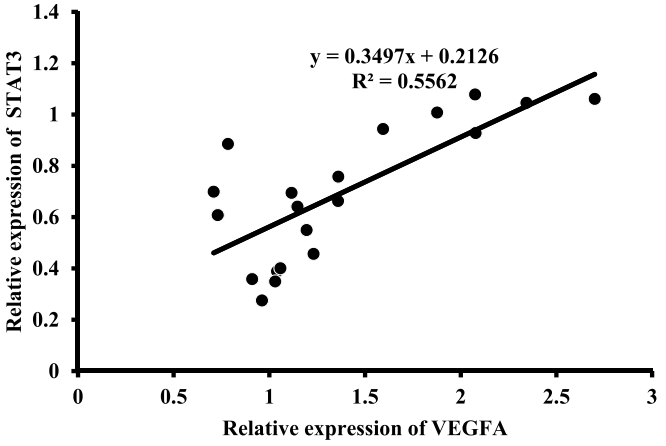

Fig. 8. The relationships of mRNA relative expression between *STAT3* and *VEGFA*.

increased by 6 times after 3 hours of hypoxia, indicating that acute hypoxia is indeed a potential inducer of *VEGF* expression (Baptista et al., 2016).

Oxidative stress, as one of environmental factors, can play a role in epigenetic regulation by modifying DNA methylation. DNA methylation is a form of epigenetic modification that affects Smyd1a, cyp19a1a, and foxl2 genes (Si et al., 2016; Wu et al., 2018). In this study, DNA methylation levels of *STAT3* gene and *VEGFA* gene were analyzed under different hypoxic conditions. The methylation level of *STAT3* 5′UTR region was significantly lower than that of control group at 3h and 6h hypoxia, indicating that hypoxia could reduce the methylation level of *STAT3* 5′UTR region. There was no significant difference in the methylation level of *STAT3* promoter region under four different hypoxia times, this indicating that hypoxia did not affect the methylation level of *STAT3* promoter region. The expression level of *STAT3* gene was negatively correlated with the methylation level of *STAT3* 5′UTR region, this indicating that hypoxia could affect the expression of *STAT3* gene by affecting the methylation level of *STAT3* 5′UTR region.

The methylation level of *VEGFA* promoter region was significantly lower than that of the control group at 3h and 6h hypoxia, this indicating that hypoxia could reduce the methylation level of *VEGFA* promoter region. The methylation level of *VEGFA* promoter region was strongly negatively correlated with the expression of *VEGFA*, this suggesting that hypoxia could affect the expression of *VEGFA* gene by affecting the methylation level of *VEGFA* promoter region. Moreover, four CpG sites (−445, −447, −522, −611) were found to be important regulatory sites by single CpG site analysis.

A previous study found the activation of *STAT3* in the reconstruction of blood vessels after injury (Li et al., 2006). This suggests that *STAT3* activation may play an important role in vascular remodeling. In tumor cells, *STAT3* acts as a transcription factor, and activation of *STAT3* can up-regulate the expression of *VEGF* (Niu et al., 2002). In this study, there was a strong positive correlation between the expression of *STAT3* and the expression of *VEGFA* under different hypoxic conditions, indicating that hypoxia could activate the *STAT3* gene in Japanese flounder, thus inducing the expression of *VEGFA* gene.

Lack of oxygen can cause changes in a series of biochemical indicators of organisms. Studies have shown that hypoxic stimulates the release of glutamate, and lactate dehydrogenase (LDH) acts as a cytotoxic marker. When an organism is exposed to acute hypoxic stress, the activity of LDH is significantly enhanced (Li et al., 2018; Maiti et al., 2006). Therefore, the contents of LDH, ALP, AST and ALT in skeletal muscle tissues of Japanese flounder were detected. In skeletal muscle LDH activity detection results show that in addition to the lack of oxygen 3 h, the rest of the group of LDH vigor and often oxygen group was no significant difference, this indicating that acute hypoxia can affect gram-negative skeletal muscle LDH vigor, but in low oxygen 6 h rapid return to oxygen levels, that were in skeletal muscle LDH has strong ability to adapt. The activity of AST and ALT increased significantly at hypoxia 6h, 24h and 48h, and ALT at hypoxia 3h, 24h and 48h, respectively, indicating that AST and ALT had certain adaptability to hypoxic conditions, but compared with LDH, the adaptability of AST and ALT in hypoxic conditions was lower than LDH. Hypoxia adversely affected AST and ALT activity. In acute hypoxia, LDH, AST and ALT showed a significant upward trend, but the trend of ALP was contrary. Hypoxia decreased the activity of ALP, and ALP activity returned to normoxic level after reoxygenation ($P > 0.05$), it indicating that ALP in skeletal muscle has a strong adaptability to hypoxia.

Angiogenic factors and their receptors promote immunosuppression by acting directly on innate and adaptive immune cells and indirectly by influencing endothelial cells (Hirsch et al., 2020). *VEGF-A* is an immunosuppressive factor that induces accumulation of regulatory T cells and inhibits T cell function by regulating immune cells (Morgane et al., 2021). Studies have shown that serum *VEGF* is positively correlated with tissue *VEGF* (Ali et al., 2011). In order to study whether hypoxia would affect the protein level of *VEGFA*, enzyme linked immunosorbent assay kit was used to detect the concentration of *VEGFA* in serum. The results showed that the concentration of *VEGFA* in serum was significantly increased after hypoxia for 6h ($P < 0.01$). Acute hypoxia can increase the concentration of *VEGFA* protein in serum, which is positively correlated with the expression of *VEGFA* mRNA in muscle tissue. It should be noted that, it compared with the significant increase of *VEGFA* mRNA in muscle tissues at 3h and 6h hypoxia, the significant increase of *VEGFA* protein concentration in serum occurred at 6h hypoxia, indicating that the increase of *VEGFA* was likely to occur in tissues first, and then produce the increase of *VEGFA* in the whole body of Japanese Flounder.

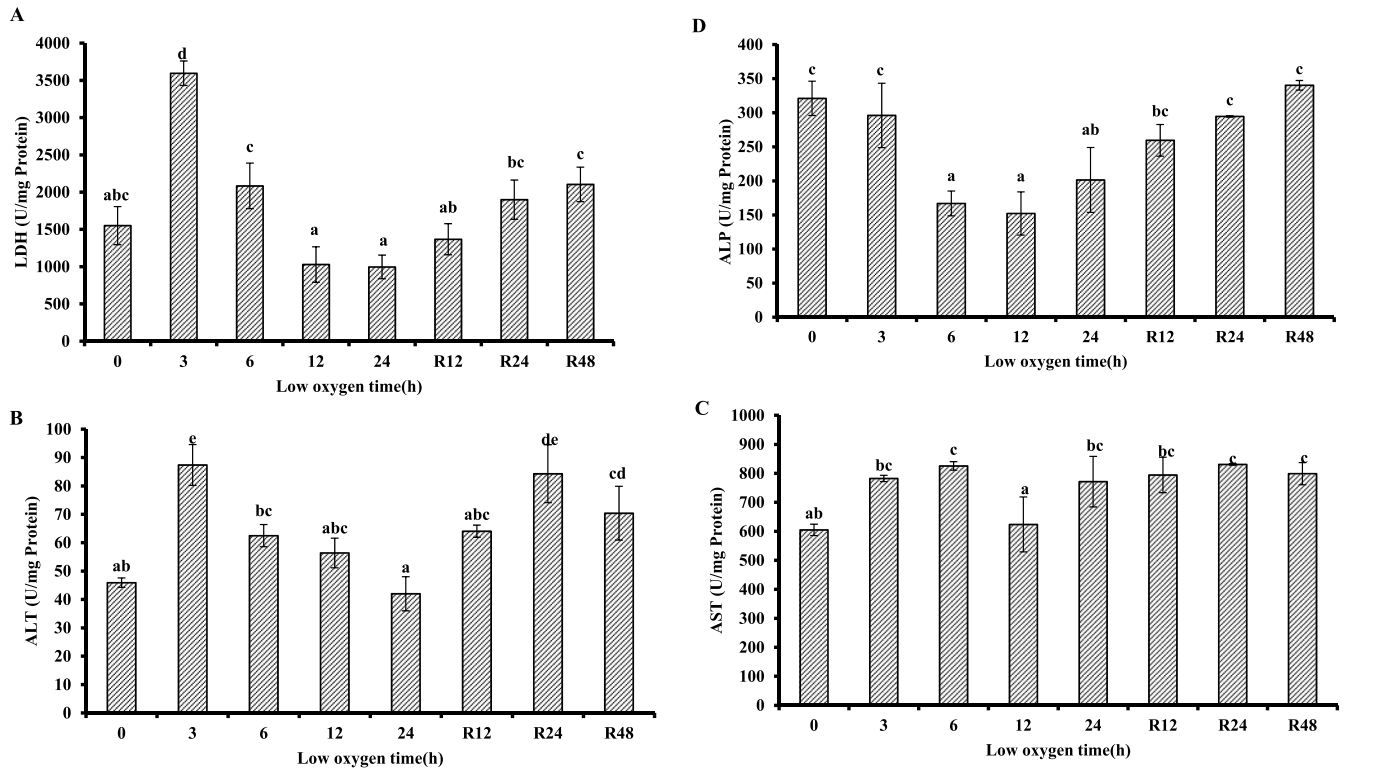

Fig. 9. Effects of acute hypoxia on activity of enzymes. Which include lactate dehydrogenase (LDH) (A), alanine aminotransferase (ALT) (B), aspartate aminotransferase (AST) (C) and alkaline phosphatase (ALP) (D) in muscle tissue homogenate. The mean values of each group were arranged in order from the smallest to the largest, marked a on the minimum mean, and then marked with letters in order of significance. Those with one same marked letter were considered insignificant, and those without the same marked letter were considered significant ($P < 0.05$).

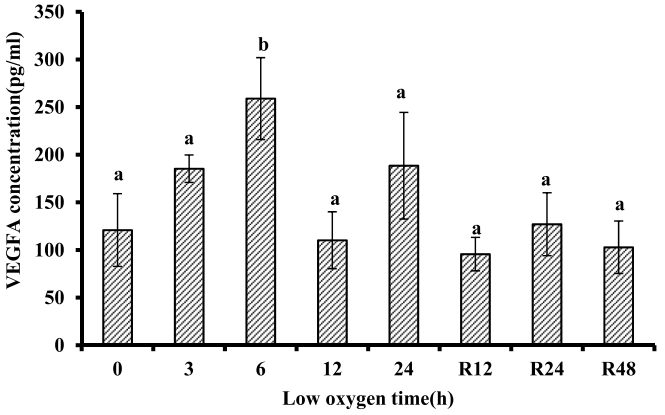

Fig. 10. Effects of acute hypoxia on serum *VEGFA* concentration in *Paralichthys olivaceus*. The mean values of each group were arranged in order from the smallest to the largest, marked a on the minimum mean, and then marked with letters in order of significance. Those with one same marked letter were considered insignificant, and those without the same marked letter were considered significant ($P < 0.05$).

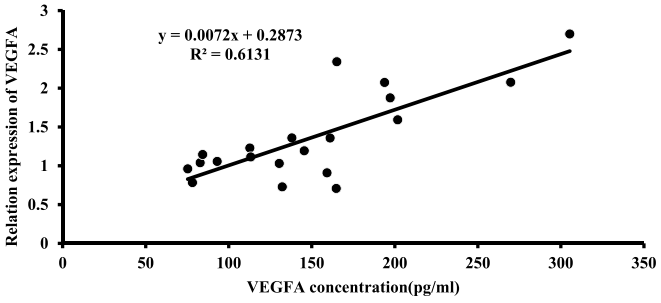

Fig. 11. Correlation between *VEGFA* protein content in serum and *VEGFA* mRNA expression in muscle.

5. Conclusion

Acute hypoxic stress can activate the *STAT3/VEGFA* signaling pathway and promote the expression of *VEGFA* by upregulating the expression of *STAT3*, thus causing the immune response of Japanese flounder. It is also affected by DNA methylation levels during regulation. In summary, environmental factors regulate biological phenotypes by activating signaling pathways, including DNA methylation modification and transcription factor regulation. This findings provide a basis for further research on hypoxia and immune signaling pathways.

Declaration of competing interest

We declare that there are no competing interests in this study.

Acknowledgments

This work was supported by the National Nature Science Foundation of China (31672642), Key Laboratory of Mariculture of Ministry of Education, Ocean University of China (No. KLM2018009) and Natural Science Foundation of Shandong Province, China (ZR2014CM018). Editors and reviewers are highly appreciated for their comments to greatly improve our manuscript.

References

Abdel-Tawwab, M., Hagras, A.E., Elbaghdady, H., Monier, M.N., 2015. Effects of dissolved oxygen and fish size on Nile tilapia, Oreochromis niloticus (L.): growth performance, whole-body composition, and innate immunity. Aquacult. Int. 23, 1261–1274.

Ali, E.M., Sheta, M., Mohsen, M., 2011. Elevated serum and tissue VEGF associated with poor outcome in breast cancer patients. Alexandria. J. Med. 47, 217–224.

Aravindan, N., Williams, M.T., Riedel, B., Shaw, A.D., 2010. Transcriptional responses of rat skeletal muscle following hypoxia-reoxygenation and near ischaemia-reperfusion. Acta Physiol. Scand. 183, 367–377.

Baptista, R.B., Souza-Castro, N., Almeida-Val, V., 2016. Acute hypoxia up-regulates HIF-1α and VEGF mRNA levels in Amazon hypoxia-tolerant Oscar (Astronotus ocellatus). Fish Physiol. Biochem. 42, 1–12.

Bautista, L., Castro, M.J., Lopez-Barneo, J., Castellano, A., 2009. Hypoxia inducible factor-2alpha stabilization and maxi-K+ channel beta1-subunit gene repression by hypoxia in cardiac myocytes: role in preconditioning. Circ. Res. 104, 1364.

Cao, Q., Zhang, T., Zhang, J., 2015. Correlation analysis of STAT3 and VEGF expression and eosinophil infiltration in nasal polyps. Eur. Arch. Oto-Rhino-Laryngol. 272, 1955–1960.

Cheng, W., Li, C.H., Chen, J.C., 2004. Effect of dissolved oxygen on the immune response of Haliotis diversicolor supertexta and its susceptibility to Vibrio parahaemolyticus. Aquaculture 232, 103–115.

Christou, H., Yoshida, A., Arthur, V., Morita, T., Kourembanas, S., 1998. Increased vascular endothelial growth factor production in the lungs of rats with hypoxia-induced pulmonary hypertension. Am. J. Respir. Cell Mol. Biol. 18, 768–776.

Ellen, B., Kechun, T., Mark, O., Amy, K., Peter, W., 2008. Skeletal muscle capillarity during hypoxia: VEGF and its activation. High Alt. Med. Biol. 9, 158–166.

Feil, R., Fraga, M.F., 2012. Epigenetics and the environment: emerging patterns and implications. Nat. Rev. Genet. 13, 97–109.

Gera, N., Tzafra, C., Stela, G., Zoya, P., 1999. Vascular endothelial growth factor (VEGF) and its receptors. Faseb. J. 13, 9–22.

He, J., Yu, Y., Qin, X.W., Zeng, R.Y., He, J.G., 2019. Identification and functional analysis of the Mandarin fish (Siniperca chuatsi) hypoxia-inducible factor-1α involved in the immune response. Fish Shellfish Immunol. 92, 141–150.

Hirsch, L., Flippot, R., Escudier, B., Albiges, L., 2020. Immunomodulatory roles of VEGF pathway inhibitors in renal cell carcinoma. Drugs 80, 789–802.

Hwang, S., Seong, H., Ryu, J., Jeong, J.Y., Han, Y.S., 2020. Phosphorylation of STAT3 and ERBB2 mediates hypoxiainduced VEGF release in ARPE19 cells. Mol. Med. Rep. 22, 2733–2740.

Ijichi, A., Sakuma, S., Tofilon, P., 1995. Hypoxia-induced vascular endothelial growth factor expression in normal rat astrocyte cultures. Glia 14, 87–93.

Jin, K., Zhu, Y., Sun, Y., Xiao, O.M., Greenberg, D.A., 2002. Vascular endothelial growth factor stimulates neurogenesis in vitro and in vivo. Proc. Natl. Acad. Sci. Unit. States Am. 99, 11946–11950.

Jr, D.J., 1997. STATs and gene regulation. Science 277, 1630–1635.

Kanda, S., Okubo, K., Oka, Y., 2011. Differential regulation of the luteinizing hormone genes in teleosts and tetrapods due to their distinct genomic environments–insights into gonadotropin beta subunit evolution. Gen. Comp. Endocrinol. 173, 253–258.

Kosmidou, I., Xagorari, A., Roussos, C., Papapetropoulos, A., 2001. Reactive oxygen species stimulate VEGF production from C2C12 skeletal myotubes through a PI3K/Akt pathway. Am. J. Physiol. Lung Cell Mol. Physiol. 280, 585–592.

Li, B., Yu, Z., Qian, G., Qian, P., Jiang, J., Wang, G., Bai, C., 2006. SOCS3 was induced by hypoxia and suppressed STAT3 phosphorylation in pulmonary arterial smooth muscle cells. Respir. Physiol. Neurobiol. 152, 83–91.

Li, M., Wang, X., Qi, C., Li, E., Du, Z., Qin, J.G., Chen, L., 2018. Metabolic response of Nile tilapia (Oreochromis niloticus) to acute and chronic hypoxia stress. Aquaculture 495, 187–195.

Li, X., Wang, T., Yin, S., Zhang, G., Cao, Q., Wen, X., Zhang, H., Wang, D., Zhu, W., 2019. The improved energy metabolism and blood oxygen-carrying capacity for pufferfish, Takifugu fasciatus, against acute hypoxia under the regulation of oxygen sensors. Fish Physiol. Biochem. 45, 323–340.

Livak, K.J., Schmittgen, T.D., 2001. Analysis of relative gene expression data using real-time quantitative PCR. Methods 25, 402–408.

Maiti, P., Singh, S.B., Sharma, A.K., Muthuraju, S., Ilavazhagan, G., 2006. Hypobaric hypoxia induces oxidative stress in rat brain. Neurochem. Int. 49, 709–716.

Minchenko, A., Bauer, T., Salceda, S., Caro, J., 1994. Hypoxia stimulation of vascular endothelial growth factor expression in vitro and in vivo. Lab. Invest. 71, 374–379.

Morgane, B., Juliette, P., Isabelle, G.F., Magali, T., 2021. Direct and indirect modulation of T cells by VEGF-A counteracted by anti-angiogenic treatment. Front. Immunol.

Nam, S.-E., Haque, M.N., Lee, J.S., Park, H.S., Rhee, J.-S., 2020. Prolonged exposure to hypoxia inhibits the growth of Pacific abalone by modulating innate immunity and oxidative status. Aquat. Toxicol. 227.

Niu, G., Wright, K.L., Huang, M., Song, L., Haura, E., Turkson, J., Zhang, S., Wang, T., Sinibaldi, D., Coppola, D., 2002. Constitutive Stat3 activity up-regulates VEGF expression and tumor angiogenesis. Oncogene 21, 2000–2008.

Ortega, S., Ondo-Méndez, A., Garzón, R., 2017. STAT3 activation by hypoxia in in vitro models of cervix cancer and endothelial cells. Biomedica 37, 119–130.

Sarma, P., Ramaiah, M.J., Pal, D., Bhadra, U., Bhadra, M.P., 2016. A novel bisindole-PBD conjugate inhibits angiogenesis by regulating STAT3 and VEGF in breast cancer cells. Life Sci. 151, 264–276.

Si, Y., Ding, Y., He, F., Wen, H., Li, J., 2016. DNA methylation level of cyp19a1a and Foxl2 gene related to their expression patterns and reproduction traits during ovary development stages of Japanese flounder (Paralichthys olivaceus). Gene 575, 321–330.

Soldatov, A.A., 2012. On the issue of classification of the hypoxia states of the aquatic organisms. Hydrobiol. J. 48, 3–17.

Stark, G.R., Kerr, I.M., Williams, B.S., Schreiber, R.H., D, R., 1998. HOW cells respond to interferons. Annu. Rev. Biochem. 67, 227–264.

Taylor, C.T., Colgan, S.P., 2017. Regulation of immunity and inflammation by hypoxia in immunological niches. Nat. Rev. Immunol. 17, 774–785.

Tian, Y., Wen, H., Qi, X., Zhang, X., Li, Y., 2018. Identification of mapk gene family in Lateolabrax maculatus and their expression profiles in response to hypoxia and salinity challenges. Gene 684, 20–29.

Turkowski, K., Brandenburg, S., Mueller, A., Kremenetskaia, I., Vajkoczy, P., 2017. VEGF as a modulator of the innate immune response in glioblastoma. Glia 66, 1–14.

Turkson, J., Bowman, T., Garcia, R., Caldenhoven, E., Groot, R.D., Jove, R., 1998. Stat3 activation by src induces specific gene regulation and is required for cell transformation. Mol. Cellular Biol. 18, 2545–2552.

Wang, M., Zhang, W., Crisostomo, P., Markel, T., Meldrum, K.K., Fu, X.Y., Meldrum, D. R., 2007. STAT3 mediates bone marrow mesenchymal stem cell VEGF production. J. Mol. Cell. Cardiol. 42, 1009–1015.

Wang, G.S., Qian, G.S., Zhou, D.S., Zhao, J.Q., 2013. JAK–STAT signaling pathway in pulmonary arterial smooth muscle cells is activated by hypoxia. Cell Biol. Int. 29, 598–603.

Wu, R.S.S., 2002. Hypoxia: from molecular responses to ecosystem responses. Mol. Cellular Biol. 45, 35–45.

Wu, S., Huang, Y., Li, S., Wen, H., Zhang, M., Li, J., Li, Y., Shao, C., He, F., 2018. DNA methylation levels and expression patterns of Smyd1a and Smyd1b genes during Metamorphosis of the Japanese Flounder (Paralichthys olivaceus). Comp. Biochem. Physiol. B Biochem. Mol. Biol. 223, 16–22.

Wu, J., Weisshaar, N., Hotz-Wagenblatt, A., Madi, A., Cui, G., 2020. Skeletal muscle antagonizes antiviral CD8 + T cell exhaustion. Science Advances 6, eaba3458.

Xu, Q., Briggs, J., Park, S., Niu, G., Kortylewski, M., Zhang, S., Gritsko, T., Turkson, J., Kay, H., Semenza, G.L., 2005. Targeting Stat3 blocks both HIF-1 and VEGF expression induced by multiple oncogenic growth signaling. pathways. Oncogene 24, 5552–5560.

Yang, J., Jing, Y., Liu, B., 2018. Targeting VEGF/VEGFR to modulate antitumor immunity. Front. Immunol. 9, 978.